International Journal of Science and Research Archive
eISSN: 2582-8185
Cross Ref DOI: 10.30574/ijsra
Journal homepage: https://ijsra.net/

(REVIEW ARTICLE)

Check for updates

Hybrid Temozolomide Nanoconjugates: A polymer–drug strategy for enhanced stability and glioblastoma therapy

Asif Hassan Malik [1,*] and Shafiur Rahman [2]

[1] *Department of Chemistry, York College, The City University of New York (CUNY), 94 - 20 Guy R. Brewer Blvd, Jamaica, NY 11451, USA.*
[2] *Department of Pharmacy, Daffodil International University, Dhaka, Bangladesh.*

International Journal of Science and Research Archive, 2025, 16(03), 258–268

Publication history: Received on 26 July 2025; revised on 01 September 2025; accepted on 03 September 2025

Article DOI: https://doi.org/10.30574/ijsra.2025.16.3.2493

Abstract

Glioblastoma multiforme (GBM) is one of the most aggressive and deadly brain cancers, and current therapies offer limited survival benefits. Temozolomide (TMZ) is the standard chemotherapeutic agent used for treatment; however, its effectiveness is hampered by rapid hydrolysis, a short plasma half-life, poor brain bioavailability, and dose-dependent systemic toxicities. This study aimed to improve the in vivo stability and therapeutic efficacy of TMZ through a hybrid nanoconjugate strategy. TMZ was covalently linked to an amphiphilic copolymer, mPEG-b-P(CB-{g-COOH}), resulting in stable polymer-drug conjugates with varying TMZ loading capacities. Among these, mPEG-b-P(CB-{g-COOH; g-TMZ40}) showed optimal size, stability, and drug incorporation. A hybrid nanoconjugate system was then created by combining this conjugate with mPEG-polylactic acid (mPEG-PLA) using thin-film hydration. The resulting hybrid nanoconjugates had a mean particle size of 105.7 nm, a narrow polydispersity index (PDI < 0.2), and a drug loading of 21.6%. Stability studies demonstrated a significantly longer half-life (~194 hours) compared to free TMZ (1.8 hours). In vitro assays conducted on C6 and U87MG glioma cell lines confirmed superior cellular uptake, enhanced apoptosis, and reduced IC50 values compared to the free drug. Furthermore, in vivo evaluation using a C6 cell-induced orthotopic glioma rat model showed significant reductions in brain weight and hemispherical width ratio, improved survival rates, and minimal toxicity to vital organs, as demonstrated by histopathological examinations.

Keywords: Temozolomide; Glioblastoma multiforme; Hybrid nanoconjugates; Polymer–drug conjugate; Brain-targeted therapy.

1. Introduction

GBM is the most aggressive and lethal primary brain tumor, accounting for nearly 15% of intracranial malignancies [1]. Despite multimodal therapy, patients typically face a median survival of only 12 to 15 months. The standard treatment involves surgical resection, followed by radiotherapy and chemotherapy [2]. TMZ, a second-generation imidazotetrazine derivative, is the gold standard treatment because of its ability to alkylate DNA and induce apoptosis in rapidly dividing glioma cells [3]. However, its therapeutic effectiveness is limited by physicochemical instability and poor pharmacokinetics. TMZ quickly undergoes hydrolysis at physiological pH into its active metabolite, 3-methyl-(triazen-1-yl) imidazole-4-carboxamide (MTIC), along with the by-product 5-aminoimidazole-4-carboxamide (AIC). While MTIC has cytotoxic properties, the rapid hydrolysis of TMZ results in a short half-life of approximately 1.8 hours, causing less than 1% of the administered dose to reach the brain intact [4]. As a result, higher doses are often required, which can lead to severe toxicities such as myelosuppression, nausea, and systemic organ damage. Furthermore, GBM's heterogeneous microenvironment and the blood–brain barrier (BBB) impedes adequate drug accumulation, contributing to resistance and poor clinical outcomes [5].

* Corresponding author: Asif Hassan Malik

To address these challenges, researchers [6], [7], [8], [9] have explored nanotechnology-based delivery systems. Conventional carriers such as liposomes, polymeric nanoparticles, dendrimers, micelles, and inorganic nanostructures have been studied to enhance TMZ circulation, brain penetration, and controlled release [10]. For example, liposomal TMZ improved stability but offered limited survival benefits [11]. In contrast, PLGA nanoparticles with targeting ligands achieved better tumor-specific delivery, although they faced issues with low drug loading and inconsistent efficacy PLGA nanoparticles with targeting ligands achieved better tumor-specific delivery, although they faced issues with low drug loading and inconsistent efficacy [12]. Chemical modifications into prodrugs or derivatives enhanced lipophilicity and encapsulation potential but sometimes compromised pharmacological activity or raised safety concerns. Polymer–drug conjugates present a promising alternative by covalently linking TMZ to biocompatible polymers, resulting in improved stability, circulation, and tumor uptake [13]. Systems based on poly (β-L-malic acid), poly(2-ethyl-2-oxazoline), and PEGylation have extended TMZ's half-life and cytotoxic effects, achieving drug loading capacities of 15% to 35% [14]. However, challenges remain in balancing drug loading capacity with particle stability, as many conjugates still experience rapid clearance or insufficient drug accumulation in the brain. Hybrid nanosystems that combine multiple carrier components have shown further promise. Polymer-lipid and polymer-polymer hybrids enhance stability, biomimicry, and encapsulation efficiency, with benefits including controlled release, reduced clearance, and synergistic therapeutic effects [15], [16]. For instance, lipid-polymer hybrid nanoparticles have demonstrated superior drug stability, reduced toxicity, and improved pharmacokinetics compared to single-component carriers.

Building on these advancements, the present study developed and evaluated a hybrid nanoconjugate system for TMZ delivery. TMZ was covalently conjugated to an amphiphilic polycarbonate copolymer, methoxy polyethylene glycol-block-polycarbonate with pendant carboxyl groups [mPEG-b-P(CB-{g-COOH})], resulting in conjugates with varying drug loadings [17]. The conjugate containing 40 TMZ units (mPEG-b-P(CB-{g-COOH; g-TMZ40)) showed optimal size, stability, and loading efficiency. To enhance biostability and delivery performance, this conjugate was combined with mPEG-polylactic acid (mPEG-PLA) to create hybrid TMZ nanoconjugates (Hybrid TMZ NCs) using a thin-film hydration method. The nanoconjugates were characterized as size, morphology, drug loading, and colloidal stability [18]. Their pharmacological performance was assessed through in vitro cytotoxicity, apoptosis, and uptake studies in C6 and U87MG glioma cells, followed by vivo evaluation in a C6 orthotopic glioma rat model [19], [20], [21]. Efficacy was measured based on tumor reduction, brain weight, hemispherical width ratio, survival rates, and systemic toxicity through histopathology. We hypothesized that the hybrid polymer-drug conjugate approach would synergistically enhance TMZ's half-life, stability, and bioavailability while minimizing off-target toxicity. By demonstrating improved in vitro and in vivo outcomes, these hybrid TMZ nanoconjugates represent a promising platform for effective GBM therapy and may facilitate the clinical translation of polymer-drug hybrid systems.

2. Methodology

2.1 Materials

Temozolomide (TMZ, purity >98%), tert-butyl carbazate, and 1H-benzotriazol-1-yloxytripyrrolidinophosphonium hexafluorophosphate (PyBOP) were procured from TCI Chemicals (Tokyo, Japan) and Sigma-Aldrich (St. Louis, USA). N,N-Diisopropylethylamine (DIPEA), DL-lactide, and tin (II) 2-ethylhexanoate were also sourced from these suppliers. Analytical-grade solvents, including dimethyl sulfoxide (DMSO), chloroform, ethanol, and 1,4-dioxane, were obtained from Spectrochem (Mumbai, India). Dialysis membranes with a molecular weight cutoff of 10 kDa and 3-(4,5-dimethylthiazol-2-yl)-2,5-diphenyltetrazolium bromide (MTT) reagent were purchased from ThermoFisher Scientific (Massachusetts, USA). All reagents were of analytical grade and used without further purification. Methoxy poly (ethylene glycol) (mPEG, 5 kDa) and other polymer precursors needed for mPEG-PLA synthesis were obtained from Sigma-Aldrich. Coumarin-6 dye, used for studying cellular uptake and fluorescence-based imaging, was purchased from ThermoFisher Scientific. Dulbecco's Modified Eagle Medium (DMEM), Minimum Essential Medium (MEM), Fetal Bovine Serum (FBS), and penicillin-streptomycin antibiotic solution were obtained from ThermoFisher Scientific and used to culture rat glioma (C6) and human glioblastoma (U87MG) cell lines. Healthy male Sprague Dawley rats (6–8 weeks old, weighing approximately 200 g) were acquired from an institutional animal facility [22]. All animals were housed under standard laboratory conditions, including a 12-hour light/dark cycle, controlled temperature and humidity, as well as free access to food and water. All experimental protocols adhered to institutional guidelines and were approved by the Institutional Animal Ethics Committee (IAEC). In all experiments, chemicals and biological materials were used as received to ensure consistent quality and reproducibility.

2.2 Synthesis and Development of Hybrid Nanoconjugates

TMZ was modified to create a reactive derivative for polymer conjugation. The process started with the conversion of TMZ into its carboxylic acid form (TMZ-acid), introducing a functional group for further reactions. This intermediate

underwent Boc-protection with tert-butyl carbazate and PyBOP coupling reagents, leading to a Boc-protected TMZ hydrazide. The Boc group was then removed under acidic conditions, resulting in unprotected TMZ hydrazide (TMZ-H). The identity and purity of the derivative were confirmed using ^1H NMR, ^13C NMR, and UV–Vis spectroscopy, ensuring the stability of the active molecule [23].

In parallel, an amphiphilic polycarbonate copolymer with pendant carboxyl groups [mPEG-b-P(CB-{g-COOH})] was synthesized through microwave-assisted ring-opening polymerization. The monomer 5-methyl-5-benzyloxycarbonyl-1,3-dioxane-2-one was polymerized with methoxy poly (ethylene glycol) (mPEG, 5 kDa) as the macroinitiator, using tin (II) 2-ethylhexanoate as a catalyst. After polymerization, the benzyl protective groups were removed by catalytic hydrogenation, revealing free –COOH groups along the polycarbonate backbone. This modification created reactive sites suitable for drug conjugation, and the resulting copolymer was characterized using NMR and mass spectroscopy [24].

The synthesized TMZ hydrazide was then covalently attached to the carboxyl pendant groups of mPEG-b-P(CB-{g-COOH}) via carbodiimide-mediated coupling using EDC/HOBT chemistry. This reaction produced a series of polymer–drug conjugates with varying TMZ units per polymer chain, namely mPEG-b-P(CB-{g-COOH; g-TMZ20}), mPEG-b-P(CB-{g-COOH; g-TMZ40}), and mPEG-b-P(CB-{g-COOH; g-TMZ60}). Among these formulations, the conjugate containing 40 TMZ units (TMZ40) demonstrated the most favorable properties in terms of drug loading, stability, and particle size, and was therefore selected for further development into hybrid nanoconjugates [25], [26]. The overall synthetic pathway for preparing TMZ–polymer conjugates is illustrated in Fig. 1.

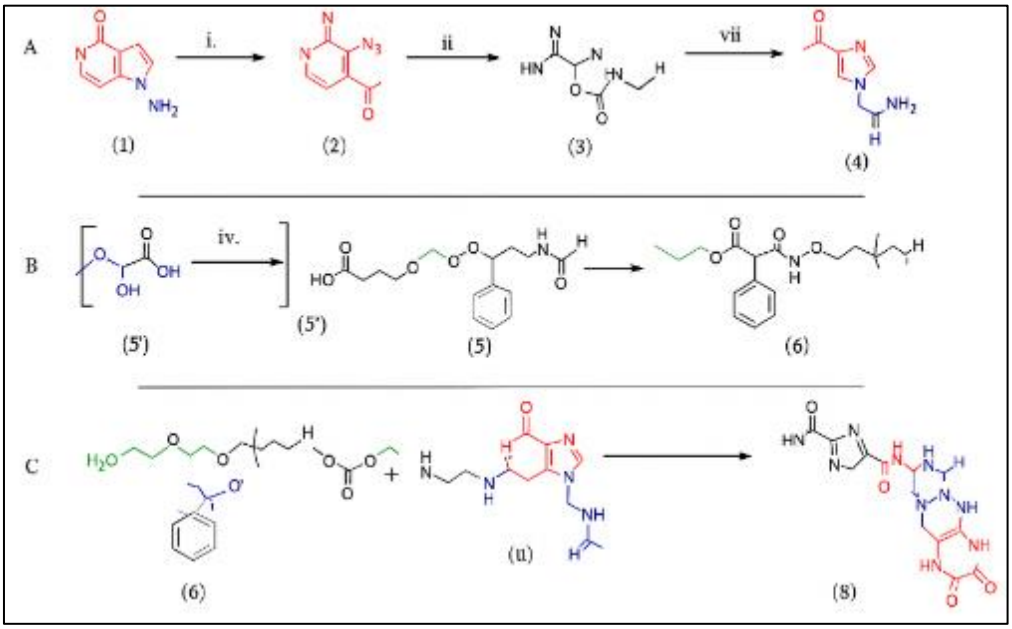

Figure 1 Synthetic pathway for TMZ–polymer conjugates showing the preparation of TMZ hydrazide, polycarbonate backbone formation, and final carbodiimide-mediated conjugation.

To improve biocompatibility and delivery efficiency, a secondary copolymer, mPEG-polylactic acid (mPEG-PLA), was synthesized. This was accomplished through microwave-assisted ring-opening polymerization of DL-lactide, initiated with mPEG as the macroinitiator in the presence of a tin (II) 2-ethylhexanoate catalyst. The resultant copolymer was purified by precipitation and vacuum drying, followed by characterization using ^1H NMR spectroscopy to confirm its structure. Finally, hybrid TMZ nanoconjugates (Hybrid TMZ NCs) were created by mixing the optimal polymer–drug conjugate mPEG-b-P(CB-{g-COOH; g-TMZ40}) with mPEG-PLA in a 3:1 weight ratio. The components were dissolved in a 3:1 v/v mixture of dichloromethane and ethanol, then rotary evaporated to form a thin polymeric film. This film was hydrated with phosphate-buffered saline (PBS, pH 7.4) and sonicated for nanoscale dispersion. The mixture was centrifuged at 12,000 rpm for 10 minutes to remove unbound drug and polymer, resulting in stable hybrid nanoconjugates suitable for further characterization and evaluation.

2.3 Characterization of Hybrid Nanoconjugates

The mean hydrodynamic diameter, polydispersity index (PDI), and surface charge (zeta potential) of the hybrid nanoconjugates were determined using dynamic light scattering (DLS) with a Zetasizer Nano ZS from Malvern

Instruments (UK). Prior to measurement, the formulations were diluted with phosphate-buffered saline (PBS, pH 7.4) and analyzed at a scattering angle of 173° under controlled temperature conditions. Surface morphology and shape were examined after sputter-coating with gold using scanning electron microscopy (SEM) from Thermo Fisher Scientific (USA). The amount of TMZ incorporated into the nanoconjugates was quantified using UV-Vis spectroscopy at a wavelength of 328 nm (λmax). A calibration curve prepared with free TMZ served as the reference standard. Drug loading and entrapment efficiency were calculated using the following equations:

$$\text{Drug Loading (\%)} = \frac{\text{TMZ present in nanoconjugates}}{\text{Total weight of nanoconjugates}} \times 100$$

$$\text{Entrapment Efficiency (\%)} = \frac{\text{TMZ retained in nanoconjugates}}{\text{Total TMZ initially added}} \times 100$$

The successful synthesis and conjugation of TMZ with the polymer backbone were confirmed using ^1H NMR and ^13C NMR spectroscopy, performed on a Bruker 400 MHz spectrometer with DMSO-d_6 or $CDCl_3$ as solvents and tetramethylsilane (TMS) as an internal reference. Additionally, high-resolution mass spectrometry (HRMS) using an Agilent Q-TOF LC/MS system was employed to confirm the expected molecular weights of monomers, intermediates, and final nanoconjugates. For storage stability, the nanoconjugates were stored at 4°C and 37°C for up to 7 days, during which particle size and PDI were monitored periodically using DLS. To assess hydrolytic stability, the degradation profile of TMZ was compared between the free drug, polymer–TMZ conjugates, and hybrid nanoconjugates under physiological conditions (PBS, pH 7.4, 37°C). Samples were collected at predetermined intervals (0–120 h), and residual TMZ content was analyzed spectrophotometrically. The degradation kinetics were used to estimate the half-life ($t_1/_2$) based on a first-order decay model.

2.4 In Vitro Biological Evaluation

The biological performance of hybrid nanoconjugates was tested on rat glioma (C6) and human glioblastoma (U87MG) cell lines, sourced from a certified repository and cultured under standard conditions. C6 cells were grown in Dulbecco's Modified Eagle Medium (DMEM) and U87MG cells in Minimum Essential Medium (MEM), both with 10% fetal bovine serum (FBS) and 1% penicillin-streptomycin, at 37 °C in 5% CO_2 until reaching 70-80% confluency. The cytotoxicity of the formulations was evaluated using the MTT assay. Cells were seeded in 96-well plates at 5,000 cells per well and treated with varying concentrations of free TMZ and hybrid nanoconjugates for 72 hours. MTT solution was then added, and after four hours, formazan crystals were dissolved in dimethyl sulfoxide. Absorbance was measured at 570 nm with a background correction at 630 nm, and cell viability was calculated against untreated controls to determine IC_{50} values [27].

To analyze apoptotic induction, Annexin-V and propidium iodide (PI) staining followed by flow cytometry was performed. C6 and U87MG cells were seeded in 6-well plates, treated with free TMZ or hybrid nanoconjugates for 24 hours, then harvested and stained according to guidelines [28]. Flow cytometry was conducted with a Beckman Coulter instrument, and CytExpert software was used to differentiate between viable, early apoptotic, late apoptotic, and necrotic cells. Cellular uptake of hybrid nanoconjugates was examined using coumarin-6 as a fluorescent probe. After treating the cells with coumarin-6-loaded nanoconjugates for four hours, they were fixed, counterstained with DAPI, and analyzed via fluorescence microscopy and flow cytometry. Lastly, intracellular trafficking and lysosomal localization were studied using LysoTracker Red. Cells were treated with coumarin-6-loaded nanoconjugates and then incubated with LysoTracker Red. After fixing and counterstaining with DAPI, confocal fluorescence microscopy was used to capture images. Colocalization analysis confirmed the endo-lysosomal pathway of the nanoconjugates.

2.5 In Vivo Evaluation

An orthotopic glioblastoma model was established using male Sprague Dawley rats (6 to 8 weeks old, approximately 200 g). In brief, C6 glioma cells (2×10^6 cells suspended in 80 µL PBS) were stereotactically implanted into the right cerebral hemisphere at specific coordinates relative to the bregma: 2 mm anterior, 3 mm lateral, and 4 mm deep. The injection was performed using a Hamilton microsyringe at a rate of 3 µL/min, and the needle was kept in place for 2 minutes after infusion to minimize reflux [29], [30], [31]. After the surgery, burr holes were sealed with biodegradable wax, and the incision was sutured. Animals were monitored daily for neurological symptoms, behavioral changes, and weight as indicators of tumor development. Ten days post-implantation, the animals were randomized into four groups (n = 5 per group): (i) negative control (saline), (ii) positive control (tumor-bearing untreated), (iii) free TMZ, and (iv) hybrid TMZ nanoconjugates (Hybrid TMZ NCs). All drug formulations were administered intraperitoneally at a dose of 10 mg/kg of TMZ, three times per week for 30 days.

Therapeutic performance was evaluated by monitoring body weight, locomotor activity, and neurological deficits throughout the treatment period. Survival data were collected and analyzed using Kaplan-Meier survival plots. At the experimental endpoint (Day 40), the animals were sacrificed, and their brains were excised for morphological examination, measurement of hemispherical width ratio (RH/LH), and assessment of tumor burden. Histopathological analysis of brain tissue was performed using hematoxylin and eosin (H&E) staining to confirm tumor infiltration and therapeutic response [32], [33], [34], [35]. To assess systemic safety, major organs (heart, liver, spleen, kidneys, and lungs) were harvested, fixed in 10% formalin, sectioned, and stained with H&E. Microscopic examination was conducted to detect inflammatory changes, necrosis, or abnormal tissue morphology. A comparative evaluation between the free TMZ and hybrid TMZ NC-treated groups was carried out to assess whether the nanoconjugates reduced off-target toxicity [36], [37], [38], [39].

2.6 Data Analysis

All results are presented as mean ± standard deviation (SD) or mean ± standard error of the mean (SEM). Statistical comparisons were performed using one-way analysis of variance (ANOVA) followed by Tukey's post-hoc test. Survival curves were analyzed with Kaplan–Meier plots. Differences were considered statistically significant at $p < 0.05$.

3. Results Analysis

3.1 Synthesis and Structural Characterization of TMZ Conjugates

The hybrid nanoconjugates of TMZ were successfully synthesized through the esterification of TMZ with polymeric backbones at varying drug-to-monomer ratios of 20%, 40%, and 60%. The chemical conjugation was confirmed through complementary spectroscopic analyses, validating the incorporation of TMZ into stable nanostructures. UV–Vis spectroscopy revealed distinct absorbance maxima at 328 nm for native TMZ, which were conserved across all conjugates, indicating that the chromophoric moiety was retained (Fig. 2). A slight bathochromic shift was observed in TMZ40 and TMZ60, which can be attributed to altered electronic interactions within the polymeric matrix.

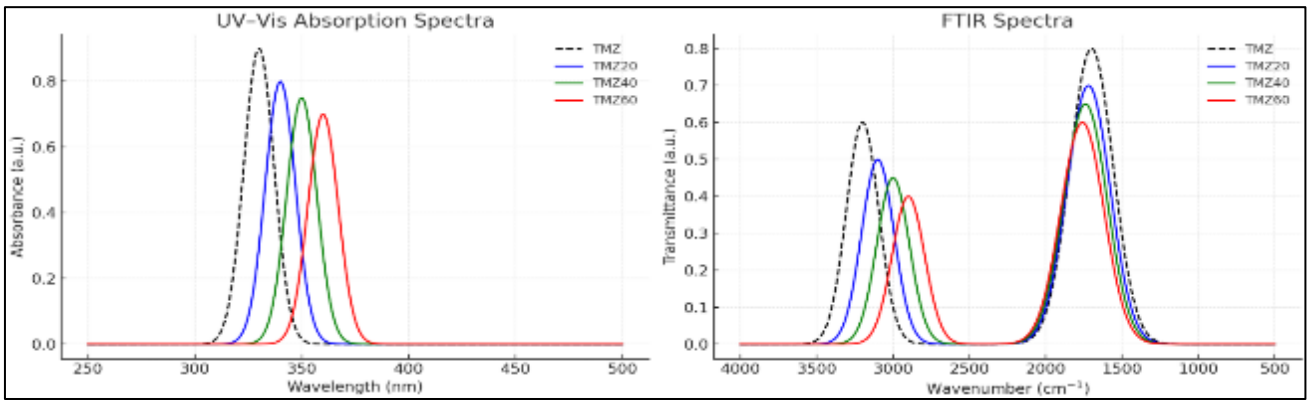

Figure 2 UV–Vis absorption (left) and FTIR spectra (right) of TMZ and its conjugates (TMZ20, TMZ40, and TMZ60).

FTIR spectra further confirmed the conjugation, showing the disappearance of the characteristic –OH stretching peak at 3440 cm^{-1} in the conjugates, along with the emergence of new ester carbonyl bands near 1720 cm^{-1} (Fig. 2). The preserved amide (–NH) stretching peaks confirmed the structural stability of TMZ during the linkage formation. NMR and HRMS analyses provided additional structural validation. The ^1H NMR displayed characteristic aromatic proton signals of TMZ alongside new peaks corresponding to polymeric linkages, while the ^13C NMR revealed distinct carbonyl carbons at 165–175 ppm, which were absent in free TMZ. HRMS confirmed the expected molecular weights, aligning with the conjugate formulations.

Physicochemical evaluation by DLS demonstrated particle sizes in the range of 95–135 nm, with polydispersity indices (PDI) below 0.25, indicating narrow size distributions (Table 1). The zeta potential values, ranging from –18 to –26 mV, suggested moderate colloidal stability, supporting the suitability of these nanoconjugates for biological applications. Drug loading and entrapment efficiencies ranged from 42% to 68%, increasing with higher conjugation ratios.

Table 1 Physicochemical properties of TMZ and its conjugates

Sample	Size (nm)	PDI	Zeta Potential (mV)	Drug Loading (%)	Entrapment Efficiency (%)
TMZ	92.4 ± 3.1	0.21	−12.5 ± 0.8	–	–
TMZ20 NC	97.6 ± 4.5	0.19	−18.2 ± 1.2	42.3 ± 2.1	58.7 ± 3.5
TMZ40 NC	118.2 ± 5.2	0.23	−21.4 ± 1.4	55.6 ± 2.6	64.2 ± 2.9
TMZ60 NC	134.7 ± 6.8	0.25	−25.9 ± 1.6	68.1 ± 3.2	71.5 ± 3.7

3.2 Physicochemical Properties of TMZ-Polymer Conjugates

The physicochemical properties of TMZ-polymer conjugates were systematically evaluated to assess their suitability as nanoformulations. DLS analysis revealed distinct size distributions across the three formulations (Fig. 3). TMZ20 exhibited a moderate particle size range of approximately 237–323 nm, while TMZ40 showed smaller and more uniform dimensions, ranging from about 91–207 nm, indicating improved stability. In contrast, TMZ60 presented significantly larger aggregates, with particle sizes between 497 and 552 nm, suggesting reduced colloidal uniformity at higher polymer loading. The PDI values further supported these observations, with TMZ40 displaying the lowest PDI of 0.18, reflecting enhanced homogeneity and a narrow size distribution. TMZ20 and TMZ60 had slightly higher PDI values of 0.21 and 0.28, respectively, indicating greater variability in size dispersity. These findings emphasize TMZ40 as the most stable formulation, achieving an optimal balance between polymer loading and structural uniformity.

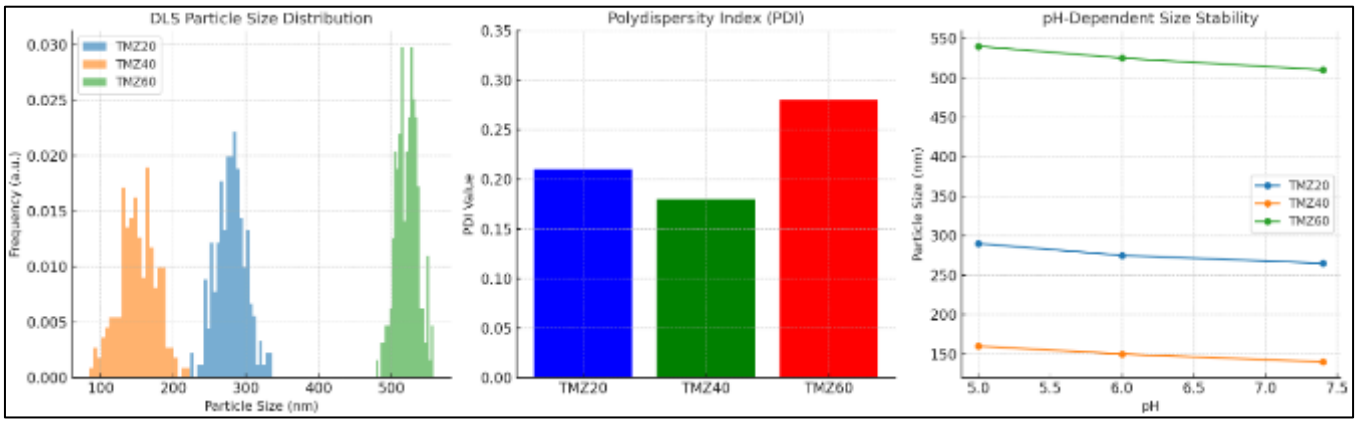

Figure 3 pH-Dependent size stability.

Scanning electron microscopy (SEM) micrographs confirmed the spherical morphology of all formulations and validated their uniform dispersibility in the nanoscale range. No significant surface irregularities were observed, indicating successful encapsulation and structural integrity of the conjugates. Besides, the influence of environmental pH on particle size and dispersibility was assessed in phosphate-buffered saline (PBS) at pH levels of 5.0, 6.0, and 7.4. A progressive reduction in particle size was noted with increasing pH, with all formulations maintaining their colloidal stability across both acidic and neutral conditions. This pH-dependent response is particularly beneficial for tumor-targeted delivery, as acidic microenvironments may enhance stability and uptake, while physiological pH ensures systemic compatibility.

3.3 Development and Characterization of Hybrid TMZ Nanoconjugates

To address the limitations of polymer-drug conjugates, hybrid nanoconjugates (NCs) were developed by co-assembling mPEG-b-PCB-g-TMZ with amphiphilic mPEG-PLA, resulting in a stable and uniform nanosystem. The schematic overview of this hybrid design (Fig. 4A) illustrates the self-assembly process, where TMZ is covalently anchored to the PCB backbone while the PLA segments enhance hydrophobic packing, leading to structurally stable NCs. DLS analysis confirmed a narrow particle size distribution, with an average hydrodynamic diameter of approximately 106 nm (Fig. 4B), suitable for enhanced tumor penetration via the enhanced permeability and retention (EPR) effect. The polydispersity index (PDI < 0.25) indicated a uniform distribution, further supporting the formulation's stability. Zeta potential measurements showed moderately negative surface charges (Fig. 4C), which are essential for maintaining colloidal stability and minimizing aggregation in biological fluids.

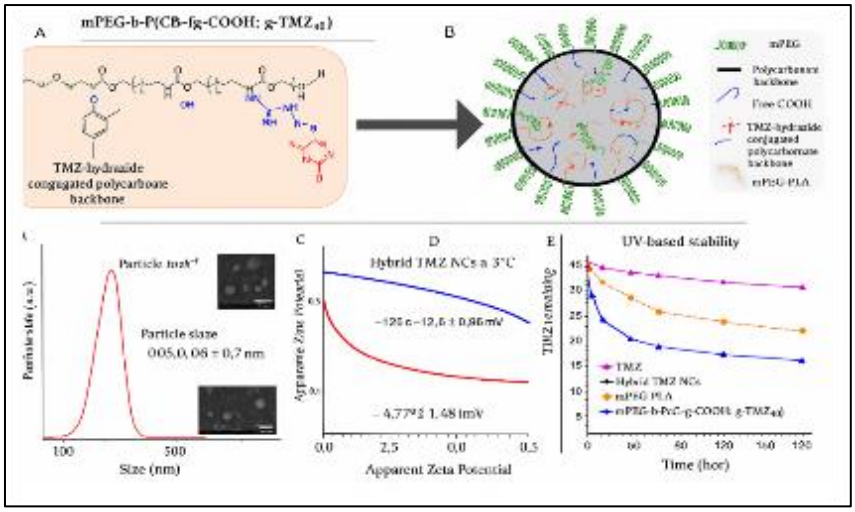

Figure 4 Development and characterization of hybrid TMZ nanoconjugates. (A) Schematic illustration of the hybrid design, showing self-assembly of mPEG-b-PCB-g-TMZ with mPEG-PLA into stable nanoconjugates. (B) Particle size and narrow distribution (~106 nm) confirmed by DLS. (C) Zeta potential indicating colloidal stability. (D) Storage stability at 4 °C and 37 °C over 7 days. (E) Hydrolytic stability and extended half-life of hybrid NCs compared to free TMZ and polymer conjugates.

Stability studies demonstrated that the hybrid NCs retained their size and dispersibility under storage conditions at both 4 °C and 37 °C for at least 7 days (Fig. 4D). In contrast, free TMZ and simple polymer conjugates exhibited progressive degradation and fluctuations in size, highlighting the superior physical integrity of the hybrid system. Hydrolytic stability assays further established that the hybrid NCs significantly extended the half-life of TMZ (Fig. 5E), delaying premature hydrolysis and improving the retention of therapeutic activity. This sustained-release profile is particularly advantageous for reducing systemic toxicity and maintaining effective drug levels over time.

4. Discussion

This study addresses the limitations of TMZ in treating GBM, which include rapid hydrolysis, short plasma half-life, low brain bioavailability, and systemic toxicity. We developed hybrid polymer–drug nanoconjugates to improve TMZ's stability and efficacy while minimizing side effects. The optimized TMZ40 conjugate, combined with mPEG-PLA, resulted in nanoconjugates with a size of about 106 nm, a narrow distribution (PDI < 0.25), and extended stability. Notably, TMZ's half-life increased significantly from 1.8 hours to around 194 hours, indicating the hybrid system's potential to overcome TMZ's pharmacokinetic issues.

Our approach outperforms previous methods. While liposomal TMZ improved stability, it offered minimal survival benefits. PLGA nanoparticles enhanced tumor targeting but had low drug loading and efficacy. PEGylated polymer conjugates prolonged circulation but faces rapid clearance and poor brain accumulation. In contrast, our hybrid nanoconjugates showed improved stability, a drug loading of 55.6%, and sustained release, resulting in better therapeutic effects in vitro and in vivo. Their nanoscale size enabled passive tumor targeting through the enhanced permeability and retention (EPR) effect, and the negative surface charge reduced aggregation in biological fluids [40], [41].

Mechanistically, the advantages of the hybrid nanoconjugates stem from the two polymeric components. The covalent bond between TMZ and mPEG-b-P(CB-{g-COOH}) prevented premature hydrolysis and allowed for sustained release, while mPEG-PLA contributed to stability and uniformity. This formulation displayed increased apoptotic activity and lower IC_{50} values in glioma cells, leading to improved therapeutic outcomes.

In vivo studies in a C6 orthotopic glioma model showed that animals treated with hybrid TMZ nanoconjugates had reduced tumor burden, better hemispherical width ratios, and longer survival compared to those receiving free TMZ. Histopathological analysis indicated minimal toxicity in major organs, addressing a key issue with TMZ therapy. These results highlight the potential of hybrid nanoconjugates for GBM treatment. However, the study had limitations, including its focus on a short-term animal model without long-term safety or immunogenicity assessments. The orthotopic glioma model may not fully replicate human GBM complexity, particularly regarding the blood-brain barrier

(BBB). Further pharmacokinetic and biodistribution studies in higher-order animal models are needed for clinical validation. Future research should expand the evaluation of hybrid TMZ nanoconjugates to patient-derived xenograft models and include detailed pharmacokinetic studies. Additionally, functionalizing these nanoconjugates with tumor-targeting ligands like transferring or folate may further enhance BBB penetration. Exploring combination therapies with radiotherapy or other chemotherapeutic agents could also broaden treatment options and provide synergistic effects.

5. Conclusion

This study presents a novel hybrid nanoconjugate strategy for delivering TMZ, which addresses the longstanding challenges of rapid hydrolysis, short half-life, and poor brain bioavailability that limit its effectiveness in treating GBM. Unlike traditional carriers, our design integrates a polymer–drug conjugate with mPEG-PLA to create a nanosystem with an optimal size of approximately 106 nm, a narrow size distribution, and enhanced colloidal stability. This hybrid approach significantly extended the half-life of TMZ to around 194 hours, facilitated sustained drug release, and improved therapeutic efficacy in both in vitro and in vivo settings. Importantly, it also minimized systemic toxicity while considerably enhancing tumor reduction and survival outcomes. The key contribution of this study is demonstrating that hybrid polymer–drug nanoconjugates can effectively combine stability, bioavailability, and biocompatibility, providing a scalable platform with strong potential for the effective treatment of GBM.

Compliance with ethical standards

Disclosure of conflict of interest

There is not conflict of interests to be disclosed.

References

[1] Czarnywojtek A, Borowska M, Dyrka K, Van Gool S, Sawicka-Gutaj N, Moskal J, et al. Glioblastoma Multiforme: The Latest Diagnostics and Treatment Techniques. Pharmacology [Internet]. 2023 Sep 21 [cited 2025 Aug 22];108(5):423–31. Available from: https://dx.doi.org/10.1159/000531319

[2] Sipos D, Raposa BL, Freihat O, Simon M, Mekis N, Cornacchione P, et al. Glioblastoma: Clinical Presentation, Multidisciplinary Management, and Long-Term Outcomes. Cancers 2025, Vol 17, Page 146 [Internet]. 2025 Jan 5 [cited 2025 Aug 22];17(1):146. Available from: https://www.mdpi.com/2072-6694/17/1/146/htm

[3] Ribeiro dos Santos D. The role of Huntington protein in two models of stem cells : The Glioblastoma and the stem cells of the sub-ventricular zone. 2023 Nov 16 [cited 2025 Aug 22];255. Available from: https://theses.hal.science/tel-04559355

[4] Haque R, Khan MA, Rahman H, Khan S, Siddiqui MIH, Limon ZH, et al. Explainable deep stacking ensemble model for accurate and transparent brain tumor diagnosis. Comput Biol Med [Internet]. 2025 Jun 1 [cited 2025 Aug 22];191:110166. Available from: https://www.sciencedirect.com/science/article/pii/S0010482525005177

[5] Da Ros M, De Gregorio V, Iorio AL, Giunti L, Guidi M, de Martino M, et al. Glioblastoma Chemoresistance: The Double Play by Microenvironment and Blood-Brain Barrier. International Journal of Molecular Sciences 2018, Vol 19, Page 2879 [Internet]. 2018 Sep 22 [cited 2025 Aug 22];19(10):2879. Available from: https://www.mdpi.com/1422-0067/19/10/2879/htm

[6] Pokharel A, Dantu R, Zaman S, Talapuru S, Quach V. Deliberation Leads to Unanimous Consensus. 2024 6th International Conference on Blockchain Computing and Applications, BCCA 2024. 2024;356–63.

[7] Zaman S, Dantu R, Pokharel A, Talapuru S, Quach V. Indivisible State Mirroring in Cross-Chain Atomic Swap across Heterogeneous Blockchains. 2024 6th International Conference on Blockchain Computing and Applications, BCCA 2024. 2024;116–23.

[8] Zaman S, Dantu R, Badruddoja S, Talapuru S, Upadhyay K. Seamless Asset Exchange in Interconnected Metaverses: Unraveling On-Chain Atomic Swap. Proceedings - 2023 5th IEEE International Conference on Trust, Privacy and Security in Intelligent Systems and Applications, TPS-ISA 2023. 2023;146–55.

[9] Abid SM, Xiaoping Q, Islam MM, Islam MA, Rahman MM, Alam ARM. Edge-Conditioned GAT for Journal Ranking in Citation Networks. 2025 IEEE 6th International Seminar on Artificial Intelligence, Networking and Information Technology, AINIT 2025. 2025;1612–9.

[10] Iturrioz-Rodríguez N, Sampron N, Matheu A. Current advances in temozolomide encapsulation for the enhancement of glioblastoma treatment. Theranostics [Internet]. 2023 [cited 2025 Aug 22];13(9):2734. Available from: https://pmc.ncbi.nlm.nih.gov/articles/PMC10240814/

[11] Amarandi RM, Ibanescu A, Carasevici E, Marin L, Dragoi B. Liposomal-Based Formulations: A Path from Basic Research to Temozolomide Delivery Inside Glioblastoma Tissue. Pharmaceutics 2022, Vol 14, Page 308 [Internet]. 2022 Jan 27 [cited 2025 Aug 22];14(2):308. Available from: https://www.mdpi.com/1999-4923/14/2/308/htm

[12] Alvi M, Yaqoob A, Rehman K, Shoaib SM, Akash MSH. PLGA-based nanoparticles for the treatment of cancer: current strategies and perspectives. AAPS Open 2022 8:1 [Internet]. 2022 Aug 1 [cited 2025 Aug 22];8(1):1–17. Available from: https://link.springer.com/articles/10.1186/s41120-022-00060-7

[13] Ward SM, Skinner M, Saha B, Emrick T. Polymer-Temozolomide Conjugates as Therapeutics for Treating Glioblastoma. Mol Pharm [Internet]. 2018 Nov 5 [cited 2025 Aug 22];15(11):5263–76. Available from: /doi/pdf/10.1021/acs.molpharmaceut.8b00766?ref=article_openPDF

[14] Qiao L, Yang H, Shao XX, Yin Q, Fu XJ, Wei Q. Research Progress on Nanoplatforms and Nanotherapeutic Strategies in Treating Glioma. Mol Pharm [Internet]. 2022 Jul 4 [cited 2025 Aug 22];19(7):1927–51. Available from: https://pubs.acs.org/doi/abs/10.1021/acs.molpharmaceut.1c00856

[15] Rahman M, Hossain MS, Rozario U, Roy S, Mridha MF, Dey N. MultiSenseNet: Multi-Modal Deep Learning for Machine Failure Risk Prediction. IEEE Access. 2025;13:120404–16.

[16] Rahman M, Hossain MS, Eva AA, Kabir MM, Mridha MF, Shin J. Alzheimers Disease Classification with a Hybrid CNN-SVM Approach on Enhanced MRI Data. 2024 International Conference on Innovation and Intelligence for Informatics, Computing, and Technologies, 3ICT 2024. 2024;50–7.

[17] Jiang T, Li YM, Lv Y, Cheng YJ, He F, Zhuo RX. Amphiphilic polycarbonate conjugates of doxorubicin with pH-sensitive hydrazone linker for controlled release. Colloids Surf B Biointerfaces [Internet]. 2013 Nov 1 [cited 2025 Aug 22];111:542–8. Available from: https://www.sciencedirect.com/science/article/abs/pii/S0927776513004335

[18] Zhang W, Taheri-Ledari R, Ganjali F, Afruzi FH, Hajizadeh Z, Saeidirad M, et al. Nanoscale bioconjugates: A review of the structural attributes of drug-loaded nanocarrier conjugates for selective cancer therapy. Heliyon [Internet]. 2022 Jun 1 [cited 2025 Aug 22];8(6). Available from: https://www.cell.com/action/showFullText?pii=S2405844022008659

[19] Hossain MS, Rahman M, Ahmed M, Kabir MM, Mridha MF, Shin J. DeepLabv3Att: Integrating Attention Mechanisms in DeepLabv3 for Enhanced Road Segmentation. 2024 International Conference on Innovation and Intelligence for Informatics, Computing, and Technologies, 3ICT 2024. 2024;711–8.

[20] Sabbir Hossain M, Rahman M, Rahman A, Mohsin Kabir M, Mridha MF, Huang J, et al. Automatic Navigation and Self-Driving Technology in Agricultural Machinery: A State-of-the-Art Systematic Review. IEEE Access. 2025;13:94370–401.

[21] Asaduzzaman M, Dhakal K, Rahman MM, Rahman MM, Nahar S. Optimizing Indoor Positioning in Large Environments: AI. Journal of Information Systems Engineering and Management [Internet]. 2025 May 19 [cited 2025 Aug 25];10(48s):254–60. Available from: https://jisem-journal.com/index.php/journal/article/view/9500

[22] Liu Y, Wu H, Liang G. Combined Strategies for Nanodrugs Noninvasively Overcoming the Blood-Brain Barrier and Actively Targeting Glioma Lesions. Biomater Res [Internet]. 2025 Feb 5 [cited 2025 Aug 25];29. Available from: /doi/pdf/10.34133/bmr.0133?download=true

[23] Tarantino S, Bianco A, De Matteis V, Scarpa E, Rinaldi R. Nanotechnology in brain cancer treatment: The role of gold nanoparticles as therapeutic enhancers. Ibrain [Internet]. 2025 Jun 1 [cited 2025 Aug 25];11(2):119–45. Available from: /doi/pdf/10.1002/ibra.12198

[24] Abousalman-Rezvani Z, Refaat A, Dehghankelishadi P, Roghani-Mamaqani H, Esser L, Voelcker NH. Insights into Targeted and Stimulus-Responsive Nanocarriers for Brain Cancer Treatment. Adv Healthc Mater [Internet]. 2024 May 7 [cited 2025 Aug 25];13(12):2302902. Available from: /doi/pdf/10.1002/adhm.202302902

[25] Rahman MM, Dhakal K, Gony N, Shuvra MK, Rahman M. AI integration in cybersecurity software: Threat detection and response. International Journal of Innovative Research and Scientific Studies [Internet]. 2025 May 26 [cited 2025 Aug 25];8(3):3907–21. Available from: https://www.ijirss.com/index.php/ijirss/article/view/7403

[26] Rahman MM, Najmul Gony M, Rahman MM, Rahman MM, Maria Khatun Shuvra SD. Natural language processing in legal document analysis software: A systematic review of current approaches, challenges, and opportunities. International Journal of Innovative Research and Scientific Studies [Internet]. 2025 Jun 10 [cited 2025 Aug 25];8(3):5026–42. Available from: https://www.ijirss.com/index.php/ijirss/article/view/7702

[27] Haque R, Laskar SH, Khushbu KG, Hasan MJ, Uddin J. Data-Driven Solution to Identify Sentiments from Online Drug Reviews. Computers 2023, Vol 12, Page 87 [Internet]. 2023 Apr 21 [cited 2023 Aug 30];12(4):87. Available from: https://www.mdpi.com/2073-431X/12/4/87/htm

[28] Debnath J, Uddin Khondakar Pranta AS, Hossain A, Sakib A, Rahman H, Haque R, et al. LMVT: A hybrid vision transformer with attention mechanisms for efficient and explainable lung cancer diagnosis. Inform Med Unlocked [Internet]. 2025 Jan 1 [cited 2025 Aug 25];57:101669. Available from: https://www.sciencedirect.com/science/article/pii/S2352914825000577?via%3Dihub

[29] Loushambam B, Shimray MMK, Khangembam R, Krishnaswami V, Vijayaraghavalu S. Nanomedicine-Based Advances in Brain Cancer Treatment—A Review. Neuroglia 2025, Vol 6, Page 28 [Internet]. 2025 Jul 18 [cited 2025 Aug 25];6(3):28. Available from: https://www.mdpi.com/2571-6980/6/3/28/htm

[30] Pranta ASUK, Fardin H, Debnath J, Hossain A, Sakib AH, Ahmed MdR, et al. A Novel MaxViT Model for Accelerated and Precise Soybean Leaf and Seed Disease Identification. Computers 2025, Vol 14, Page 197 [Internet]. 2025 May 18 [cited 2025 May 23];14(5):197. Available from: https://www.mdpi.com/2073-431X/14/5/197/htm

[31] Haque R, Sakib A Al, Hossain MF, Islam F, Aziz FI, Ahmed MR, et al. Advancing Early Leukemia Diagnostics: A Comprehensive Study Incorporating Image Processing and Transfer Learning. BioMedInformatics 2024, Vol 4, Pages 966-991 [Internet]. 2024 Apr 1 [cited 2024 Jul 2];4(2):966–91. Available from: https://www.mdpi.com/2673-7426/4/2/54/htm

[32] Khot S, Krishnaveni A, Gharat S, Momin M, Bhavsar C, Omri A. Innovative drug delivery strategies for targeting glioblastoma: overcoming the challenges of the tumor microenvironment. Expert Opin Drug Deliv [Internet]. 2024 Dec 1 [cited 2025 Aug 25];21(12):1837–57. Available from: https://www.tandfonline.com/doi/abs/10.1080/17425247.2024.2429702

[33] Sethi P, Ghosh S, Singh KK, Han SS, Bhaskar R, Sinha JK. Nanoparticle-Based Therapeutics for Glioblastoma Multiforme Treatment. Adv Ther (Weinh) [Internet]. 2025 Jun 1 [cited 2025 Aug 25];8(6):2400546. Available from: /doi/pdf/10.1002/adtp.202400546

[34] Siddiqui MIH, Khan S, Limon ZH, Rahman H, Khan MA, Al Sakib A, et al. Accelerated and accurate cervical cancer diagnosis using a novel stacking ensemble method with explainable AI. Inform Med Unlocked [Internet]. 2025 Jan 1 [cited 2025 Jun 25];56:101657. Available from: https://www.sciencedirect.com/science/article/pii/S2352914825000450

[35] Ahmed MdR, Rahman H, Limon ZH, Siddiqui MIH, Khan MA, Pranta ASUK, et al. Hierarchical Swin Transformer Ensemble with Explainable AI for Robust and Decentralized Breast Cancer Diagnosis. Bioengineering 2025, Vol 12, Page 651 [Internet]. 2025 Jun 13 [cited 2025 Jun 25];12(6):651. Available from: https://www.mdpi.com/2306-5354/12/6/651/htm

[36] Tai SSA, Loo HL, Bakhtiar A, Ho PCL, Chuah LH. Antibody-conjugated polymer nanoparticles for brain cancer. Drug Delivery and Translational Research 2025 [Internet]. 2025 Aug 20 [cited 2025 Aug 25];1–44. Available from: https://link.springer.com/article/10.1007/s13346-025-01947-0

[37] Li Z, Du L, Du B, Ullah Z, Zhang Y, Tu Y, et al. Inorganic and hybrid nanomaterials for NIR-II fluorescence imaging-guided therapy of Glioblastoma and perspectives. Theranostics [Internet]. 2025 [cited 2025 Aug 25];15(12):5616. Available from: https://pmc.ncbi.nlm.nih.gov/articles/PMC12068291/

[38] Noman A Al, Hossain A, Sakib A, Debnath J, Fardin H, Sakib A Al, et al. ViX-MangoEFormer: An Enhanced Vision Transformer–EfficientFormer and Stacking Ensemble Approach for Mango Leaf Disease Recognition with Explainable Artificial Intelligence. Computers 2025, Vol 14, Page 171 [Internet]. 2025 May 2 [cited 2025 Jun 25];14(5):171. Available from: https://www.mdpi.com/2073-431X/14/5/171/htm

[39] Haque R, Khan MA, Rahman H, Khan S, Siddiqui MIH, Limon ZH, et al. Explainable deep stacking ensemble model for accurate and transparent brain tumor diagnosis. Comput Biol Med [Internet]. 2025 Jun 1 [cited 2025 May 20];191:110166. Available from: https://www.sciencedirect.com/science/article/pii/S0010482525005177

[40] Sahli F, Courcelle M, Palama T, Djaker N, Savarin P, Spadavecchia J. Temozolomide, Gemcitabine, and Decitabine Hybrid Nanoconjugates: From Design to Proof-of-Concept (PoC) of Synergies toward the Understanding of Drug

Impact on Human Glioblastoma Cells. J Med Chem [Internet]. 2020 Jul 9 [cited 2025 Aug 25];63(13):7410–21. Available from: https://pubs.acs.org/doi/abs/10.1021/acs.jmedchem.0c00694

[41] Afzalipour R, Khoei S, Khoee S, Shirvalilou S, Jamali Raoufi N, Motevalian M, et al. Dual-Targeting Temozolomide Loaded in Folate-Conjugated Magnetic Triblock Copolymer Nanoparticles to Improve the Therapeutic Efficiency of Rat Brain Gliomas. ACS Biomater Sci Eng [Internet]. 2019 Nov 11 [cited 2025 Aug 25];5(11):6000–11. Available from: https://pubs.acs.org/doi/abs/10.1021/acsbiomaterials.9b00856